Tracking neutrophils in zebrafish: the use of synthetic data sets

Constantino Carlos Reyes-Aldasoro[1]
c.c.reyes-aldasoro@sussex.ac.uk
Katy Henry [2]
k.henry@sheffield.ac.uk
Stephen A. Renshaw[2]
s.a.renshaw@sheffield.ac.uk

[1] Biomedical Engineering School of Engineering and Informatics University of Sussex, UK

[2] MRC Centre for Developmental and Biomedical Genetics, and Department of Infection and Immunity, University of Sheffield, UK

Abstract

In this work we present a series of data sets that model the behaviour of neutrophils as observed with a confocal microscope. The data sets describe important characteristics of the migration of neutrophils such as collisions and path tortuosity as well as different levels of background noise. Neutrophil trajectories were manually defined, and Gaussian shapes similar to those of real data sets were assigned to each position of a neutrophil. The availability of synthetic data sets such as the ones proposed here, together with appropriate *gold standards* will benefit those wanting to test the robustness and accuracy of segmentation and tracking algorithms.

1 Introduction

The advent of multiphoton and confocal fluorescence microscopy, which allows 3D imaging of specimens *in vivo* with high spatial and temporal resolution, has been widely adopted in the Life Sciences [6] for applications ranging from the observation of microvascular permeability [11], the assessment of mitochondrial function [15], and examining tumour angiogenesis [13], to the observation of neutrophil apoptosis and migration [3]. Confocal and multiphoton microscopes capture the intensity value (i) at a specific three dimensional location (x y z). This intensity is related to the photons detected at the camera, which are in turn related to the structure or concentration of a substance within the sample which can present different fluorescent reactions to the excitation frequency (f). As the observation is repeated over time (t), the data becomes a 5-dimensional matrix i x y z f t (Fig. 1a). Thus, the data acquired on a single experiment can easily be of many gigabytes (GB) and special considerations have to be implemented for the storage and transport of such data sets.

Zebrafish larvae have emerged as a key model organism in recent years, with a unique combination of advantages over other model systems for the detailed study of inflammation biology *in vivo* [9]. Their optical transparency allows visualisation of physiological and pathological processes as it is possible to visualise both the anatomy of the fish together with fluorescent cell populations *in vivo* (Fig. 1b). Genetic manipulations can be easily performed, both to genetically manipulate the inflammatory response, but also to label individual cells

with fluorescent markers [10]. This then allows these cell populations to be observed in high temporal and spatial resolutions, during inflammation resolution, using multiphoton and confocal microscopy.

The combination of confocal microscopes with zebrafish models has provided a crucial setting for the detailed study of inflammation biology [2]. Inflammation is a process critical to life itself, without it multicellular animals could not protect themselves against the threat of competing unicellular microorganisms. However, the power of our immune systems can also be a threat to our own health when inflammatory responses fail to resolve in a timely fashion. Understanding how immune cells behave during all phases of inflammation *in vivo* is an important part of understanding cellular migration and interaction. Neutrophils and macrophages (collectively termed *myeloid cells*) are the key cells of the innate immune system, and are essential aspects of both host defence against infectious disease, and tissue damage caused during inflammatory disease. The function of such cells is notoriously difficult to examine *in vivo*.

Neutrophil analysis from multiphoton data sets is complicated for several reasons. First, the data sets can be of high-resolution images as mentioned previously and thus the computational complexity is considerable. Second, neutrophil behaviour is typically analysed from derived measurements, *e.g.* velocity, shape changes or activation, rather than from direct observation. Thus it is necessary to pre-process the data: namely, to segment the neutrophils and track them in time [12] before any quantitative analysis can be performed. Third, the collisions that occur between neutrophils present a major challenge to tracking, as two separate fluorescent cells may appear as a single large fluorescent cell. The problem is further complicated by the fact that neutrophils can elongate considerably, and two pseudopods can stretch apart looking then as two separate neutrophils since the region between the two elongated pseudopods will decrease in fluorescence intensity. Fourth, *gold-standards* to evaluate the robustness of segmentation and tracking algorithms are rarely available for biomedical data, as these require considerable time from an expert user to manually annotated the data, in this case segment and track neutrophils. To the best of the authors' knowledge, there are no public data sets of neutrophils with gold-standards that can be used to compare and validate analysis algorithms. Furthermore, many labs employ proprietary software with its own routines, which makes replication and verification difficult [7] as these routines are not available to the wider community.

For this work, we generated a series of synthetic data sets in MATLAB c that simulate a group of migrating neutrophils. The neutrophils exhibit different migration behaviours, such as change in shape, collisions in their paths and different levels of tortuosity. The data sets and their trajectories are freely available [14] and can be used as a benchmark to test the robustness of segmentation and tracking algorithms for neutrophils in zebrafish.

2 Synthetic Neutrophil Data Sets

Numerous data sets of neutrophils in zebrafish were carefully observed to capture the main characteristics to be reproduced in the artificial sets. Six trajectories were manually determined by setting the *row column* positions of the centroids at every time point for 98 time frames with z-stacks of 11 slices and 550 550 pixels. Each trajectory was designed so that it would represent different neutrophil behaviours: some trajectories were very oriented and had movements with uniform distance between time frames, whilst others were less uniform and would move at different velocities, some were tortuous whilst others were straight. The

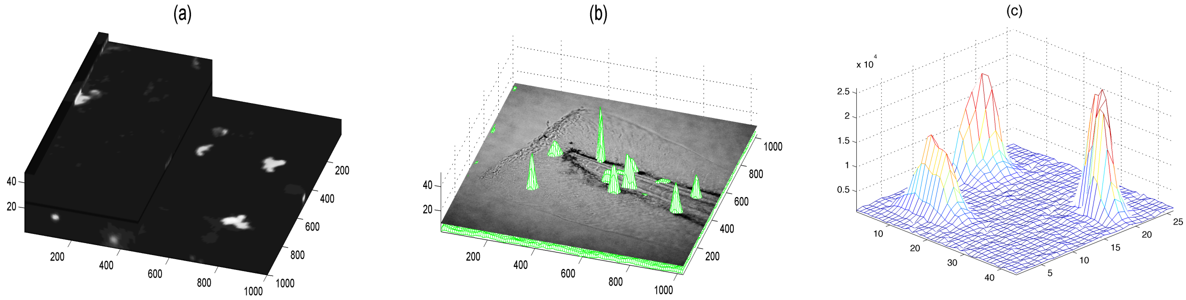

Figure 1: Fluorescent neutrophils in zebrafish: (a) One time frame t, 24 slices (1024 1024 pixels) in the z axis, two frequencies (f_1 in the top for neutrophils, f_2 in the bottom for macrophages). The data has been sliced to visualise the intensity at different levels. (b) A single fluorescent slice plotted as a mesh with intensity-related height, and one slice of the DIC image, which shows the anatomy of the fish. (c) A region of interest showing the decaying intensity of the neutrophils, which will be modelled as a Gaussian function.

trajectories of cells 1 and 2 collided several times in the second half of the time frames whilst cells 3 and 4 collided at the beginning of the movement. Cell 6 migrated without meandering and then stopped at the end (which represents the wound area of an inflammation-based experiment) whilst 5 presented a delayed activation. The neutrophils were then assigned intensities that modelled the fluorescent intensity of the neutrophils with a 3D Gaussian distribution. The orientation of the Gaussians varied according to the displacement of the artificial neutrophils, *i.e.* they were round when the cells were static, or elongated when in movement. The shapes were simplistic and in the future we plan to assign more realistic shapes with extending pseudopods.

The tracks with the Gaussians were saved as the *gold standard* and five different data sets were generated by adding varying levels of white Gaussian noise resulting in data sets with distributions with increasing similarity between the neutrophils and the background reflected by the decreasing values of the Bhattacharyya Distance (1.61, 1.25, 1, 0.66, 0.45) (Fig. 2b). The Bhattacharyya Distance (*BD*) [1, 5] is a well-known measurement of the separability between two probabilistic distributions based on their means and standard deviations.

In its simplest formulation, the Bhattacharyya distance between two classes can be calculated from the variance and mean of each class in the following way:

$$D_B \; k_1 \; k_2 \qquad \frac{1}{4}\ln \; \frac{1}{4} \; \frac{{}^{2}_{k_1}}{{}^{2}_{k_2}} \; \frac{{}^{2}_{k_2}}{{}^{2}_{k_1}} \; 2 \qquad \frac{1}{4} \; \frac{k_1 \qquad k_2}{{}^{2}_{k_1} \quad {}^{2}_{k_2}}^{2} \qquad (1)$$

where: $D_B\; k_1\; k_2$ is the Bhattacharyya distance between k_1 th and k_2 th classes, ${}_{k_1}$ is the variance of the k_1 th class, ${}_{k_1}$ is the mean of the k_1 th class, and $k_1\; k_2$ are two different training classes. For the multidimensional distance, the variances are replaced by co-variance matrices and the means become vectors [4]:

$$D_B \; k_1 \; k_2 \qquad \frac{1}{2}\ln \; \frac{\frac{1}{2} \quad {}_{k_1} \qquad {}_{k_2}}{\overline{\quad}\; {}_{k_2} \quad {}_{k_1}} \qquad \frac{1}{4} \quad {}_{k_1} \qquad {}_{k_2} \;{}^{T} \quad {}_{k_1} \qquad {}_{k_2} \;{}^{1} \quad {}_{k_1} \qquad {}_{k_2} \qquad (2)$$

where ^{T} is the transpose of the matrix. The Mahalanobis distance used in Fisher Linear Discriminant Analysis (LDA) is a particular case of the Bhattacharyya, when the variances of the two classes are equal; this would eliminate the first term of the distance.

Fig. 2c,d display one slice of the z-stack for time frame 26 for the data sets with largest *BD* (less noise) and smallest *BD* (more noise). The mean intensity values for the background and neutrophil classes were 10 and 18 respectively.

3 Segmentation and Tracking Algorithm

To test the data sets, we implemented a hysteresis segmentation and keyhole model of movement tracking algorithm as proposed in [12]. Briefly, the segmentation algorithm performed intensity-based segmentation with a hysteresis double threshold, with high and low thresholds determined based on Otsu's algorithm [8]. Volume elements (voxels) below and above the lower threshold were classified as background and neutrophils respectively. Intermediate-level voxels were classified as cells if in contact with voxels above the high threshold, or as background otherwise. Tracking was performed with a keyhole model of movement where cell movement is predicted to follow one of two possibilities: either completely random around the current position of the cell, or oriented following the same orientation and velocity as the previous jump. These options are translated into two regions of probability: a circle and a wedge, together resembling a keyhole. Several post-processing tasks were performed: initial nodes were validated with a backward linking of nodes, tracks for which neutrophils disappear for one frame were joined, small tracks were discarded, and collisions between neutrophils were detected and cells split to be re-tracked.

4 Results

The segmentation and tracking algorithms were applied to the 5 data sets described above and a sensitivity analysis for the threshold levels was performed, as this was the only input parameter that can be modified by the user. We defined two measurements of accuracy: (1) the number of tracks generated by the algorithms (Fig. 3a) and (2) the distance between the centroids of the segmented neutrophils and the *gold standard* (Fig. 3b). It was important to use both measurements as it is possible to have scenarios where tracks can be broken into several segments, each of which will be very close to the gold standard (good performance in 2, bad performance in 1) or conversely the tracking could confuse neutrophils after a collision and follow the incorrect neutrophil along the track of the gold standard (good performance in 1, bad performance in 2). The threshold values automatically calculated were 19 8 21 1 , therefore, we varied the levels from 11 to 31 for the lower threshold and 13 to 33 for the higher threshold. As it should be expected, the errors increase at the extreme values: background regions were considered neutrophils with low threshold levels, and faint neutrophils were lost with high threshold levels. However, the results are fairly stable for a good range of threshold values (19 27 for the lower threshold, shaded areas) where the number of tracks is (6 8) for all the data sets and the average distance between the centroids of the segmented neutrophils and the gold standard is 1 09 pixels.

5 Conclusions

In this work we present synthetic data sets that simulate the migration of neutrophils as observed with a confocal microscope. We tested the data sets with a segmentation and tracking algorithm which provided stable results for a large range of threshold values. In the future,

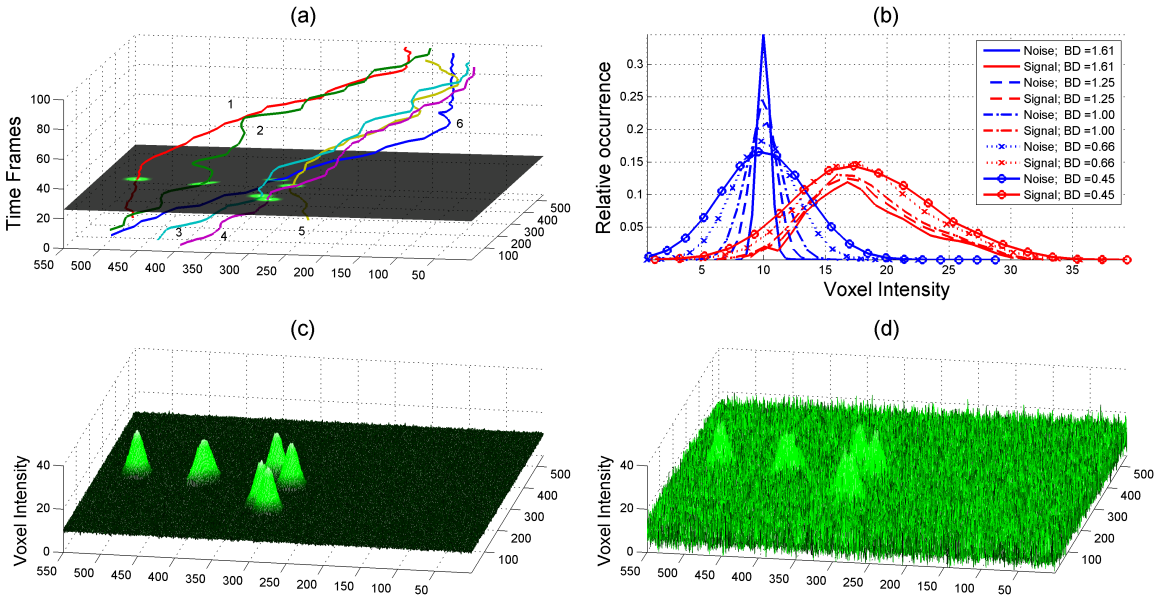

Figure 2: Synthetic data sets. (a) One slice of the intensity at time 30 and the paths of six individual neutrophils shown as coloured lines. The z-axis indicates time. (b) Five sets of histograms of the distributions for background (noise) and neutrophils (signal) for different levels of noise. The separability of the two classes is indicated by the values of the Bhattacharyya Distance (*BD*). (c) One slice of the set with $BD = 1.61$ shown as a mesh where the intensity corresponds to the z-axis. (d) One slice of the set with $BD = 0.45$. The level of the noise can be easily compared between the two data sets.

we plan to develop more data sets that describe different neutrophil behaviour characteristics as well as acquisition settings, *i.e.* different resolutions, as validation data sets to test the robustness of analysis algorithms. We also plan to create and release a function through which new tracks with different behaviours can be generated as required. The data sets and the neutrophil trajectories are freely available [14] .

References

[1] Guy B Coleman and Harry C Andrews. Image Segmentation by Clustering. *Proceedings of the IEEE*, 67(5):773–785, 1979.

[2] P. M. Elks, C. A. Loynes, and S. A. Renshaw. Measuring inflammatory cell migration in the zebrafish. *Methods Mol Biol*, 769:261–75, 2011.

[3] P. M. Elks, F. J. van Eeden, G. Dixon, X. Wang, C. C. Reyes-Aldasoro, P. W. Ingham, M. K. Whyte, S. R. Walmsley, and S. A. Renshaw. Activation of hif-1alpha delays inflammation resolution by promoting neutrophil persistence in a zebrafish inflammation model. *Blood*, 118:712–722, 2011.

[4] K. Fukunaga. *Introduction to Statistical Pattern Recognition*. Academic Press, 1972.

[5] Thomas Kailath. The divergence and bhattacharyya distance measures in signal selection. *IEEE Trans. on Commun. Technology*, 15(1):52–60, 1967.

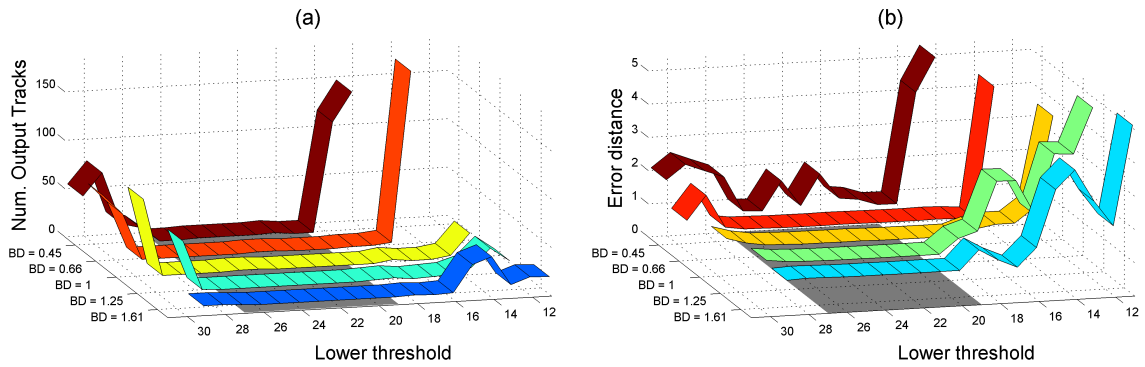

Figure 3: Validation of the algorithms against different input thresholds. (a) Number of tracks generated by the algorithms; the correct number was 6. (b) Average distance between the centroids of the segmented neutrophils and the gold standard in pixels. The shaded are denotes the range in which the algorithms provide consistent results.

[6] K. Konig. Multiphoton microscopy in life sciences. *J Microsc*, 200(Pt 2):83–104., 2000.

[7] T. A. Nielsen, H. Nilsson, and T. Matheson. A formal mathematical framework for physiological observations, experiments and analyses. *J R Soc Interface*, 2011.

[8] N. Otsu. A threshold selection method from gray level histograms. *IEEE Trans. Syst. Man Cybern.*, 9:62–66, 1979.

[9] S. A. Renshaw and N. S. Trede. A model 450 million years in the making: zebrafish and vertebrate immunity. *Disease Models & Mechanisms*, 5(1):38, 2012.

[10] S. A. Renshaw, C. A. Loynes, D. M. Trushell, S. Elworthy, P. W. Ingham, and M. K. Whyte. A transgenic zebrafish model of neutrophilic inflammation. *Blood*, 108(13): 3976–8, 2006.

[11] C. C. Reyes-Aldasoro, I. Wilson, V. E. Prise, P. R. Barber, S. M. Ameer-Beg, B. Vojnovic, V. J. Cunningham, and G. M. Tozer. Estimation of apparent tumor vascular permeability from multiphoton fluorescence microscopic images of p22 rat sarcomas in vivo. *Microcirculation*, 15(1):65–79, 2008.

[12] C.C. Reyes-Aldasoro, Y. Zhao, D. Coca, S.A. Billings, V. Kadirkamanathan, G. M. Tozer, and S. A. Renshaw. Analysis of immune cell function using in vivo cell shape analysis and tracking. In *4th IAPR Int Conf Pat Rec Bioinformatics*, Shef, UK, 2009.

[13] G. M. Tozer et al. Blood vessel maturation and response to vascular-disrupting therapy in single vascular endothelial growth factor-A isoform-producing tumors. *Cancer Res.*, 68(7):2301–2311, 2008.

[14] Webpage. http://www.neutrophil.org.uk. 2012.

[15] Z. Zhong et al. Nim811, a mitochondrial permeability transition inhibitor, prevents mitochondrial depolarization in small-for-size rat liver grafts. *American Journal of Transplantation*, 7(5):1103–1111, 2007.